



# First Assessment of GF3-02 SAR Ocean Wind Retrieval

Junxin Yang<sup>1,2,3</sup> , Bing Han<sup>1,2,\*</sup>, Lihua Zhong<sup>1,2</sup>, Xinzhe Yuan<sup>4</sup>, Xiaochen Wang<sup>1,2</sup> and Yuxin Hu<sup>1,2,3</sup> and Chibiao Ding<sup>1,2,3</sup>

<sup>1</sup> Aerospace Information Research Institute, Chinese Academy of Sciences, Beijing 100094, China; yangjunxin18@mails.ucas.ac.cn (J.Y.); lhzhong@mail.ie.ac.cn (L.Z.); wangxc@radi.ac.cn (X.W.); yxhu@mail.ie.ac.cn (Y.H.); cbding@mail.ie.ac.cn (C.D.)

<sup>2</sup> Key Laboratory of Technology in Geo-Spatial Information Processing and Application Systems, Chinese Academy of Sciences, Beijing 100190, China

<sup>3</sup> School of Electronic, Electrical and Communication Engineering, University of Chinese Academy of Sciences, Beijing 100049, China

<sup>4</sup> National Satellite Ocean Application Service, Beijing 100081, China; harley\_yuan@mail.nsoas.org.cn

\* Correspondence: han\_bing@mail.ie.ac.cn; Tel.: +86-010-5888-7208 (ext. 8956)

**Abstract:** On 23 November 2021, the Gaofen-3-02 (GF3-02) satellite was successfully launched in the Jiuquan Satellite Launch Center of China. The primary payload is C-band Synthetic Aperture Radar (SAR), with a maximum resolution of 1 m, and includes 12 imaging modes such as Spotlight, Strip, and TOPSAR, which will play an essential role in marine environment monitoring. As an important marine environmental parameter, the wind speed accuracy retrieved by GF3-02 SAR directly reflects its performance and effectiveness as an operational product. Therefore, based on the wind data of buoys of the National Data Buoy Center (NDBC), ECMWF reanalysis V5 (ERA5), and HY-2B Scatterometer (SCA), a preliminary accuracy assessment of the wind speed retrieved by GF3-02 SAR is carried out in this paper. The wind speed retrieval accuracy of GF3-02 SAR in the co-polarization (HH+VV) data under different Geophysical Model Functions (GMFs) is discussed by using 478 level-1A Single Look Complex (SLC) ocean products acquired in Quad-Polarization Strip I (QPSI) and produced by the National Satellite Ocean Application Service (NSOAS) from January to March 2022. The results show that the optimal root mean square errors (RMSE) are 1.40 m/s, 1.18 m/s, and 1.24 m/s for the VV polarization and 1.39 m/s, 1.19 m/s, and 1.52 m/s for the HH polarization compared to the NDBC wind speed, the ERA5 wind speed, and the HY-2B SCA wind speed, respectively. The preliminary results show that GF3-02 SAR has good wind speed retrieval ability and can meet the needs of operational products.

**Keywords:** GF3-02; SAR; sea surface wind; CMOD



**Citation:** Yang, J.; Han, B.; Zhong, L.; Yuan, X.; Wang, X.; Hu, Y.; Ding, C. First Assessment of GF3-02 SAR Ocean Wind Retrieval. *Remote Sens.* **2022**, *14*, 1880. <https://doi.org/10.3390/rs14081880>

Academic Editor: Antonio Iodice

Received: 6 March 2022

Accepted: 11 April 2022

Published: 14 April 2022

**Publisher's Note:** MDPI stays neutral with regard to jurisdictional claims in published maps and institutional affiliations.



**Copyright:** © 2022 by the authors. Licensee MDPI, Basel, Switzerland. This article is an open access article distributed under the terms and conditions of the Creative Commons Attribution (CC BY) license (<https://creativecommons.org/licenses/by/4.0/>).

## 1. Introduction

As an important marine environmental parameter, the sea surface wind field affects ocean dynamic processes such as sea wave formation, water mass composition, and wave motion. In recent years, the research on the efficient and high-precision acquisition method of wind field information on the vast ocean surface has become a research direction of great concern in marine environmental monitoring and the development and utilization of marine resources. The development of Synthetic Aperture Radar (SAR) plays a vital role in the remote sensing of ocean surface characteristics. It can carry out all-weather high-resolution and large-area dynamic monitoring of the global surface. The SAR-derived normalized radar cross-sections (NRCS) on the sea surface are mainly caused by Bragg scattering [1], which is caused by the resonance interaction between the magnetic wave emitted by the radar and the centimeter-scale short wave, and is mainly related to the radar parameters and the characteristics of the sea surface. In recent years, scholars in ocean remote sensing worldwide have carried out much extensive research on the

characteristics of SAR wind field retrieval based on microwave scatterometer wind field retrieval algorithm.

At present, Geophysical Model Function (GMF) is the most widely used wind speed retrieval algorithm, an empirical formula that combines the NRCS with the wind speed and direction at 10 m above sea level and the incident angle of the radar. The CMOD series models suitable for C-band VV polarization data are the most mature. According to the scatterometer data, CMOD2 [2], CMOD4 [3], CMOD-IFR2 [4], CMOD5 [5], CMOD5.N [6], C2013 [7], CMOD5.H [8], CMOD7 [9], etc. have been developed successively. For HH polarization, the HH polarization NRCS is transformed into VV polarization NRCS by polarization ratio (PR), and then the GMFs mode function of VV polarization is used to retrieve the sea surface wind speed. For example, Elfouhaily [10], Thompson [11], and Zhang et al. [12] put forward the PR formula only related to the incident angle. Ren et al. [13] obtained a PR model suitable for Gaofen-3 (GF-3) SAR by fitting the  $\alpha$  parameter of the PR model proposed by Thompson through GF-3 dual-polarization data. Mouche et al. [14] found that the polarization ratio PR is modulated by the relative wind direction. According to this property, they proposed a PR model related to the incident angle and the relative wind direction. Similarly, Wang Lei [15] used GF-3 SAR data to establish a PR model related to the incident angle and relative wind direction. In recent decades, these GMFs models have been successfully applied to the retrieval of wind speed by C-band satellites such as ERS-1/2 [16], ENVISAT ASAR, Radarsat-1/2, Sentinel-1A/B, and GF-3. Fan et al. [17] used CMOD-IFR2 to retrieve the wind speed from the ENVISAT ASAR image, and root mean square errors (RMSE) of the retrieval wind speed and the NCEP/QSCAT mixed wind vector were 1.9 m/s and 1.6 m/s, respectively. Zhang et al. [18] compared the RMSE of wind speed retrieval of Radarsat-2 by different GMFs, and considered CMOD5 to be the optimal wind speed retrieval model. Monaldo et al. [19] used CMOD5.N to verify the wind speed of the Sentinel-1A SAR image, and the RMSE of the estimated wind speed and ASCAT scatterometer wind field product was 1.42 m/s. Wang et al. [20] used the GF-3 SAR data to retrieve the wind field and compared it with the buoy wind field data. The results showed that the wind speed RMSE was 2.46 m/s and the wind direction RMSE was 22.22°. With the accumulation of SAR data, CSARMOD [21], CSARMOD2 [22], and CMODH [23] models are developed using SAR data. In [23], Zhang not only proposed a CMODH model for SAR HH polarization data, which we call CMODH\_HH in this paper, but also derived a set of model coefficients suitable for VV polarization data, which we called CMODH\_VV. It is shown in [24] that the CMODH-retrieved wind speeds are in good agreement with the buoy measurements, with an RMSE of 1.66 m/s for Radarsat-2 and 2.05 m/s for Sentinel-1A/B. In short, with the accumulation of sea surface remote sensing data, more and more accurate GMFs are proposed, which provides a guarantee for marine applications.

On 23 November 2021, China successfully launched a 1-meter resolution C-band SAR satellite, also known as Gaofen-3 02 (GF3-02), at the Jiuquan Satellite Launch Center. The satellite is China's first SAR operational satellite, marking the transformation of the SAR satellite business from scientific experiment to business application, further enhancing China's operational observation capabilities for marine remote sensing. The satellite operates in a solar synchronous regression orbit at 755 km. The primary payload is C-band SAR, with a maximum resolution of 1 m, and includes 12 imaging modes such as Spotlight, Strip, and TOPSAR. Together with the GF-3 SAR satellite [25], it forms the constellation of China's ocean surveillance and monitoring satellites. The satellite revisit and coverage capabilities have been significantly improved, marking the initial formation of China's ocean surveillance and monitoring satellite constellation.

The purpose of this paper is to show the first wind speed retrieval results of GF3-02 SAR and to preliminarily verify the sea surface wind speed retrieval capability of GF3-02 SAR. Section 2 introduces the GF3-02 SAR data and wind field data used and the classical co-polarization wind speed retrieval model. The wind speed retrieval results and discussions for each model are given in Section 3. Then, Section 4 discusses the sources of wind speed

retrieval errors and the comparison of ERA5 wind speeds and HY-2B SCA wind speeds with NDBC buoy wind speeds. Finally, Section 5 gives the conclusions.

## 2. Materials and Method

### 2.1. GF3-02 SAR Data

The GF3-02 SAR products used in this paper are all produced by the National Satellite Ocean Application Service (NSOAS), which has the production capacity of SAR products for the first time. As shown in Table 1, we have collected 520 GF3-02 SAR products acquired in Quad-Polarization Strip I (QPSI) from January to March 2022. Among them, 478 scenes are for the ocean scenes whose incidence angle is from 20° to 50°, and there are two sets of data for the Amazon rainforest with orbit ID 1153 and 1427. The map of collected GF3-02 SAR ocean imagery location is shown in Figure 1. The ocean scene locations are mainly concentrated in the waters off the Hawaiian Islands and the waters off the west coast of the United States. Since the radiometric calibration of GF3-02 has not been completed, we used the Amazon rainforest data to obtain the calibration constant of the images. The calibration constants for HH polarization obtained from two sets of Amazon rainforest data with different beam codes are 13.60 dB and 13.52 dB, respectively, and 13.82 dB and 14.00 dB for VV polarization. As the link gain of different beam codes is considered in the radiometric correction process, it shows that the calibration constant of QPSI mode image produced by NSOAS is independent of beam code. We take the scaling constant as 13.56 dB for HH polarization and 13.91 dB for VV polarization. Furthermore, the QPSI imaging mode and capability are as follows: the resolution is 8 m, the swath is 30 km, and HH, HV, VH, and VV polarization data can be obtained simultaneously.

**Table 1.** GF3-02 SAR sea surface data collected.

Orbit ID	Beam Code	Center Incident Angle (°)	Imaging Time	Num of Products Used	Area
914	189	19.99	2022-01-25	28	Ocean
1216	192	25.38	2022-02-15	21	Ocean
1614	192	26.56	2022-03-14	26	Ocean
1153	195	30.41	2022-02-10	18	Rainforest
870	197	32.34	2022-01-22	22	Ocean
1616	197	33.28	2022-03-15	20	Ocean
964	198	33.73	2022-01-28	24	Ocean
879	198	33.82	2022-01-22	31	Ocean
1607	199	36.23	2022-03-14	32	Ocean
1614	199	36.22	2022-03-14	43	Ocean
1427	200	37.46	2022-03-01	24	Rainforest
899	201	37.75	2022-01-24	4	Ocean
916	202	38.56	2022-01-25	11	Ocean
899	206	41.76	2022-01-24	36	Ocean
892	209	44.03	2022-01-23	39	Ocean
1238	209	44.02	2022-02-16	33	Ocean
1629	209	44.62	2022-03-15	25	Ocean
1629	211	46.03	2022-03-15	39	Ocean
1634	213	47.41	2022-03-16	27	Ocean
1620	215	48.73	2022-03-15	17	Ocean

### 2.2. Buoy Data

The wind in-site measurements of the buoys have been collected from the National Data Buoy Center (NDBC) of the National Oceanic and Atmospheric Administration (NOAA), which are used as the ground truth to evaluate the accuracy of the GF3-02 SAR wind speed retrieval results. Due to the limited number of scenes that the collected SAR ocean data covers the NDBC buoy, we chose to match the nearest SAR image within 50 km of the buoy for research. There are a total of 10 matching data located in the waters off

the Hawaiian Islands and the waters off the west coast of the United States, as shown in Figure 2.

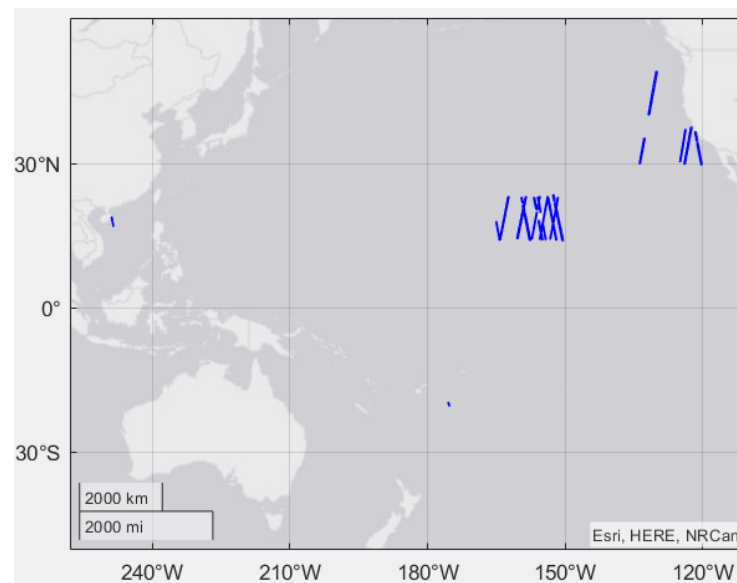


**Figure 1.** The map of collected GF3-02 SAR ocean imagery location.

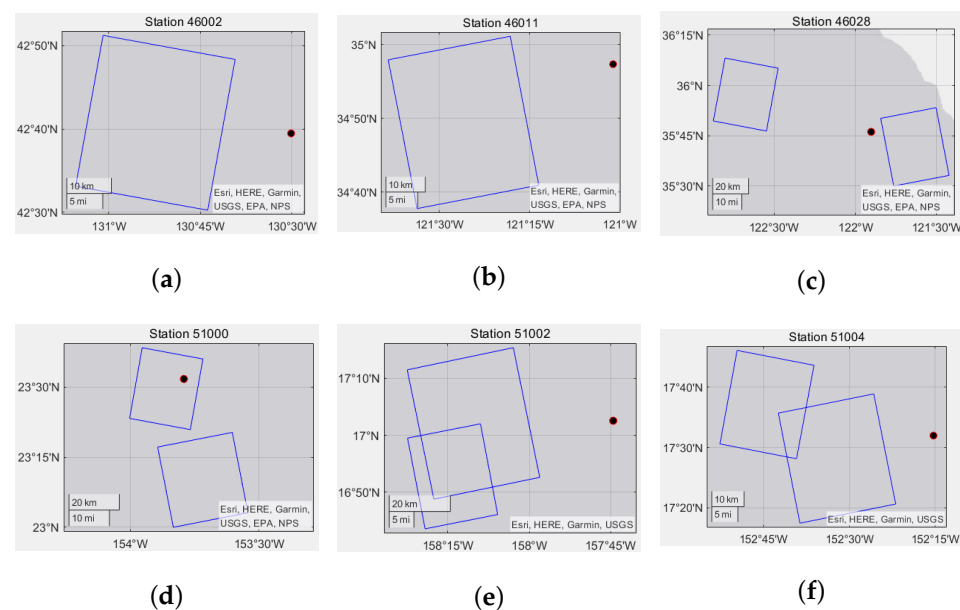


**Figure 2.** The map of matched GF3-02 SAR ocean scene (blue box) in NDBC's (a) Station 46002, (b) Station 46011, (c) Station 46026, (d) Station 51000, (e) Station 51002, (f) Station 51004. The black dots represent the locations of NDBC buoys.

### 2.3. ERA5 Data

ERA5 wind data matched with the imaging time and irradiation area of SAR data are also used for sea surface wind field retrieval and verification. ERA5 is the fifth generation of European Centre for Medium-Range Weather Forecasts (ECMWF) global climate reanalysis data, which provides hourly estimates of numerous atmospheric, wave, and surface quantities. The wind data for reanalysis has been re-divided into a regular latitude and longitude grid of 0.25 degrees.

#### 2.4. HY-2B Scatterometer Data

The HY-2B satellite is equipped with a Ku-band scatterometer (HSCATB), which is mainly used for global sea surface wind field measurements. The HY-2B satellite ground data processing system is constructed and managed by the NSOAS. The 25 km along-orbit grid wind field products (L2B-level data) of the HY-2B satellite scatterometer (SCA) are distributed to users around the world. According to the product introduction of HY-2B, its wind speed measurement accuracy is 2 m/s, and the effective wind speed measurement range is 2 m/s to 24 m/s. A total of 213 scenarios of GF3-02 SAR data are matched in this paper, and space-time matching with SCA wind products is carried out, and the time interval is within 1 h.

#### 2.5. Wind Speed Retrieval Model

The NRCS of sea surface SAR data depends on the radar incidence angle, wind speed, and direction. The NRCS is generally described by nonlinear formulas related to the angle of incidence, wind speed, and relative wind direction (the angle between the radar-observed wind direction and the wind direction). Taking CMOD5.N as an example [6], the nonlinear formula is as follows:

$$\sigma_0(v, \phi, \theta) = B_0(v, \theta)(1 + B_1(V, \theta) \cos(\phi) + B_2(v, \theta) \cos(2\phi))^p, \quad (1)$$

where the isotropic term  $B_0$ , the upwind/downwind amplitude  $B_1$  and the upwind/crosswind amplitude  $B_2$  are all the functions of wind speed  $v$  and incident angle  $\theta$ . The  $\phi$  is relative wind direction and the  $p$  is a constant with a value of 1.6. Different models were used to evaluate the wind speed retrieval capability of GF3-02 SAR for VV polarization, including the CMOD\_IFR2, CMOD5, CMOD5.N, CSARMOD2 and CMODH\_VV models.

For HH polarization, an additional PR model is generally required to convert HH polarization NRCS to VV polarization NRCS. PR is defined as

$$PR = \sigma_0^{VV} / \sigma_0^{HH}, \quad (2)$$

where  $\sigma_0^{VV}$  and  $\sigma_0^{HH}$  are the NRCS in linear units for VV and HH polarization, respectively. This paper adopts the polarization ratio formula related to the incident angle proposed by Elfouhaily, Zhang, Ren, and Wang. At the same time, the HH polarization model of CMODH\_HH is used to evaluate the wind speed retrieval capability of GF3-02 SAR for HH polarization, which can directly retrieve wind speed from HH polarization NRCS without relying on the PR model.

### 3. Results

First, the GF3-02 SAR image is averaged in the azimuth of 1km and the range of 1 km in the center of the scene, and matched with the ERA5 data in space and time, where matched ERA5 wind speed range is 0 m/s to 12 m/s. Second, the ERA5 wind direction data is used as the input of the GMFs model to obtain the wind speed retrieved by the GF3-02 SAR. Finally, it is verified by comparing the NDBC, ERA5, and HY-2B SCA wind speeds.

#### 3.1. GF3-02 SAR Wind Speed from VV Polarization

##### 3.1.1. Compared with NDBC Wind Speed

Figure 3a shows the comparison between wind speed retrieval results from GF3-02 SAR VV polarization data using CMOD\_IFR2, CMOD5, CMOD5.N, CSARMOD2, and CMODH\_VV models and the matched NDBC wind speed. Among them, the abscissa is the wind speed of NDBC, and the ordinate is the wind speed retrieved by the GF3-02 SAR. The RMSE of GF3-02 SAR wind speed retrieval results are 2.03 m/s, 1.78 m/s, 1.40 m/s, 1.82 m/s, and 1.63 m/s, respectively. Based on this, the GF3-02 SAR wind speed retrieval results using the CMOD5.N model are optimal with an RMSE of 1.40 m/s. Furthermore, compared with the proposed retrieval model based on SAR data, the RMSE of the CMODH\_VV is 1.63 m/s, which is better than those of the CSARMOD2.

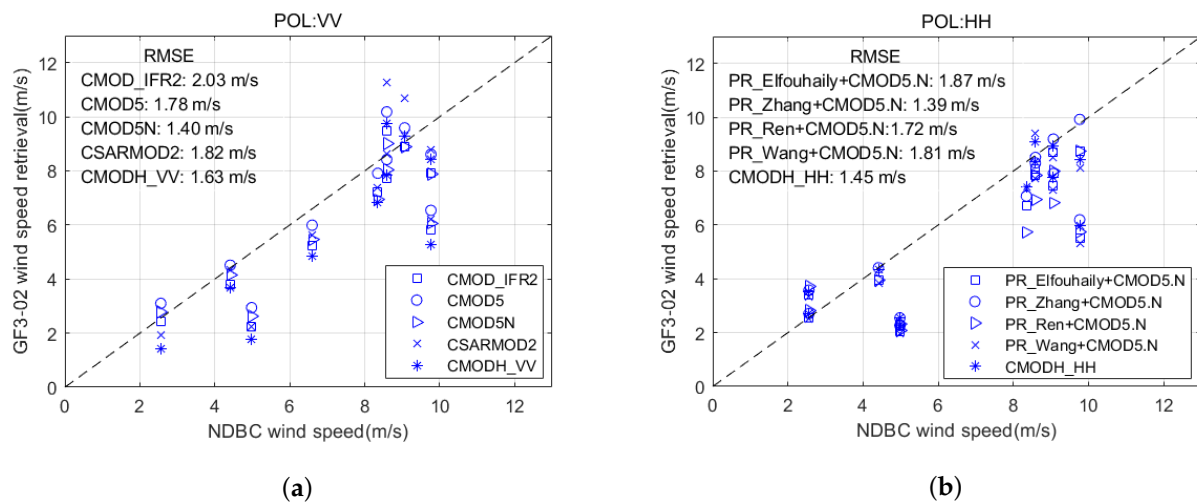


**Figure 3.** Comparison of wind speed retrieval results of the GF3-02 SAR data based on each GMF model and NDBC speed wind. (a) VV polarization; (b) HH polarization.

### 3.1.2. Compared with ERA5 Wind Speed

Figure 4 shows a comparison of the wind speeds retrieved from GF3-02 VV polarization data and the ERA5 wind speeds. Among them, the abscissa is the wind speed of ERA5, and the ordinate is the wind speed retrieved by the GF3-02 SAR. Table 2 is the wind speed retrieval accuracy of GF3-02 VV polarization data based on each GMF model compared with ERA5 wind speed. The RMSE of the retrieved wind speeds are 1.53 m/s, 1.35 m/s, 1.18 m/s, 1.50 m/s, and 1.32 m/s, respectively. It can be clearly seen that with CMOD5.N, the RMSE is also the smallest, the deviation is 0.03 m/s, and the correlation coefficient is 0.84. Furthermore, the RMSE of the CMODH\_VV is 1.32 m/s and the correlation coefficient is 0.83, which are also better than those of the CSARMOD2.

**Table 2.** Comparison of wind speed retrieval results of the GF3-02 VV polarization data based on each GMF model and ERA5 wind data.

GMFs	Bias (m/s)	RMSE (m/s)	Corr
CMOD_IFR2	−0.83	1.53	0.83
CMOD5	−0.67	1.35	0.84
CMOD5.N	0.03	1.18	0.84
CSARMOD2	−0.19	1.50	0.82
CMODH_VV	−0.61	1.32	0.83

### 3.1.3. Compared with HY-2B SCA Wind Speed

Figure 5 shows a comparison of the wind speeds retrieved from GF3-02 VV polarization data and the HY-2B SCA wind speeds. Among them, the abscissa is the wind speed of HY-2B SCA, and the ordinate is the wind speed retrieved by the GF3-02 SAR. Table 3 is the wind speed retrieval accuracy of GF3-02 VV polarization data based on each GMF model compared with HY-2B SCA wind speed. It can be seen that the deviation is negative, which means that the SAR wind speed is generally lower than the SCA wind speed. The RMSE of the retrieved wind speeds are 1.88 m/s, 1.66 m/s, 1.24 m/s, 1.73 m/s, and 1.70 m/s, respectively. Consistent with the comparison results of buoy wind speed and ERA5 wind speed, the RMSE of CMOD5N is also the smallest, the deviation is −0.53 m/s, and the correlation coefficient is 0.80. Furthermore, the RMSE of the CMODH\_VV is 1.70 m/s and the correlation coefficient is 0.81, which are also a little better than those of the CSARMOD2.

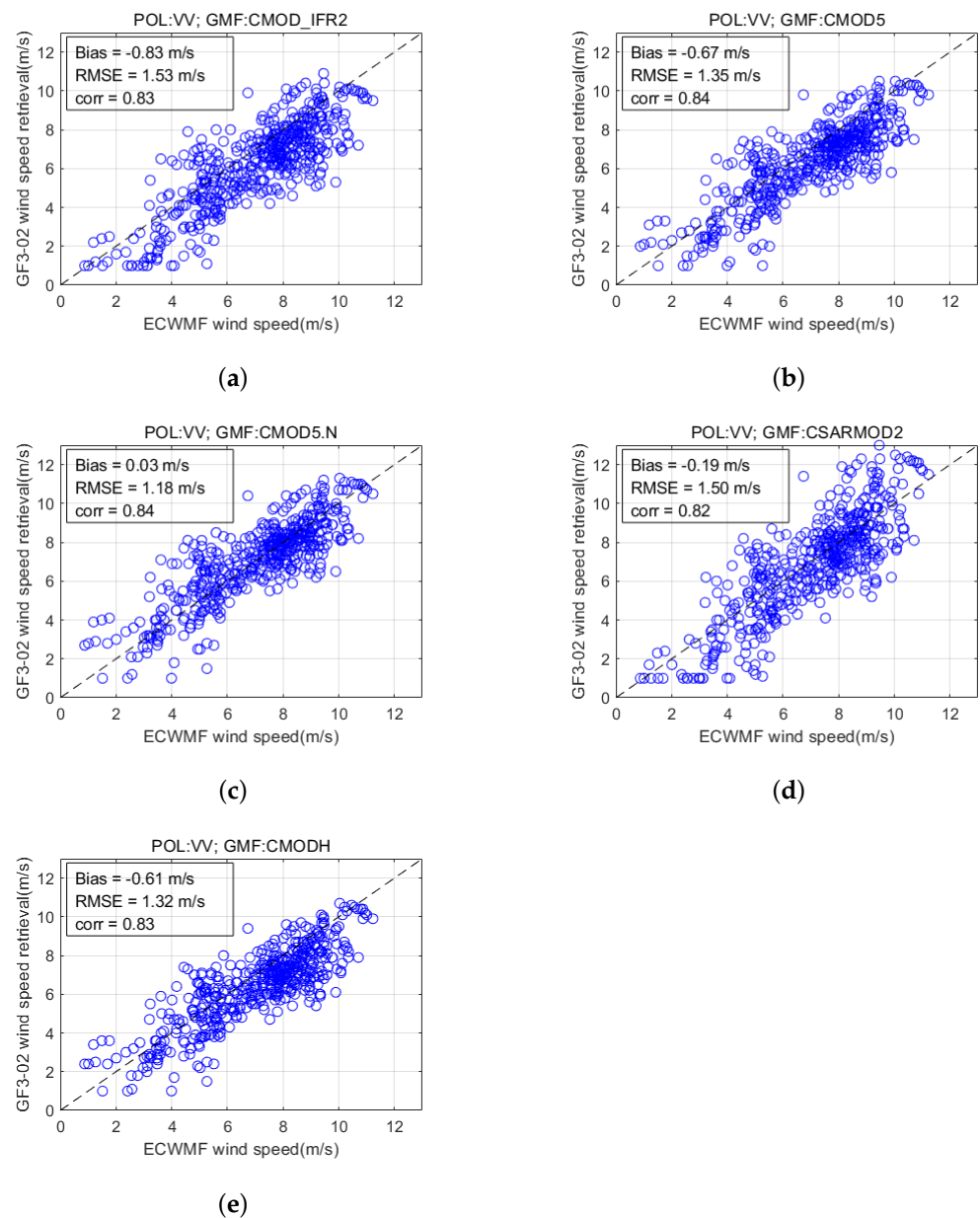


**Figure 4.** Comparison of wind speed retrieval results from GF3-02 VV polarization data based on (a) CMOD\_IFR2, (b) CMOD5, (c) CMOD5.N, (d) CSARMOD2, and (e) CMODH\_VV and ERA5 wind data.

**Table 3.** Comparison of wind speed retrieval results of the GF3-02 VV polarization data based on each GMF model and HY-2B SCA wind speed.

GMFs	Bias (m/s)	RMSE (m/s)	Corr
CMOD_IFR2	-1.34	1.88	0.77
CMOD5	-1.23	1.66	0.80
CMOD5.N	-0.53	1.24	0.80
CSARMOD2	-0.72	1.73	0.79
CMODH_VV	-1.36	1.70	0.81

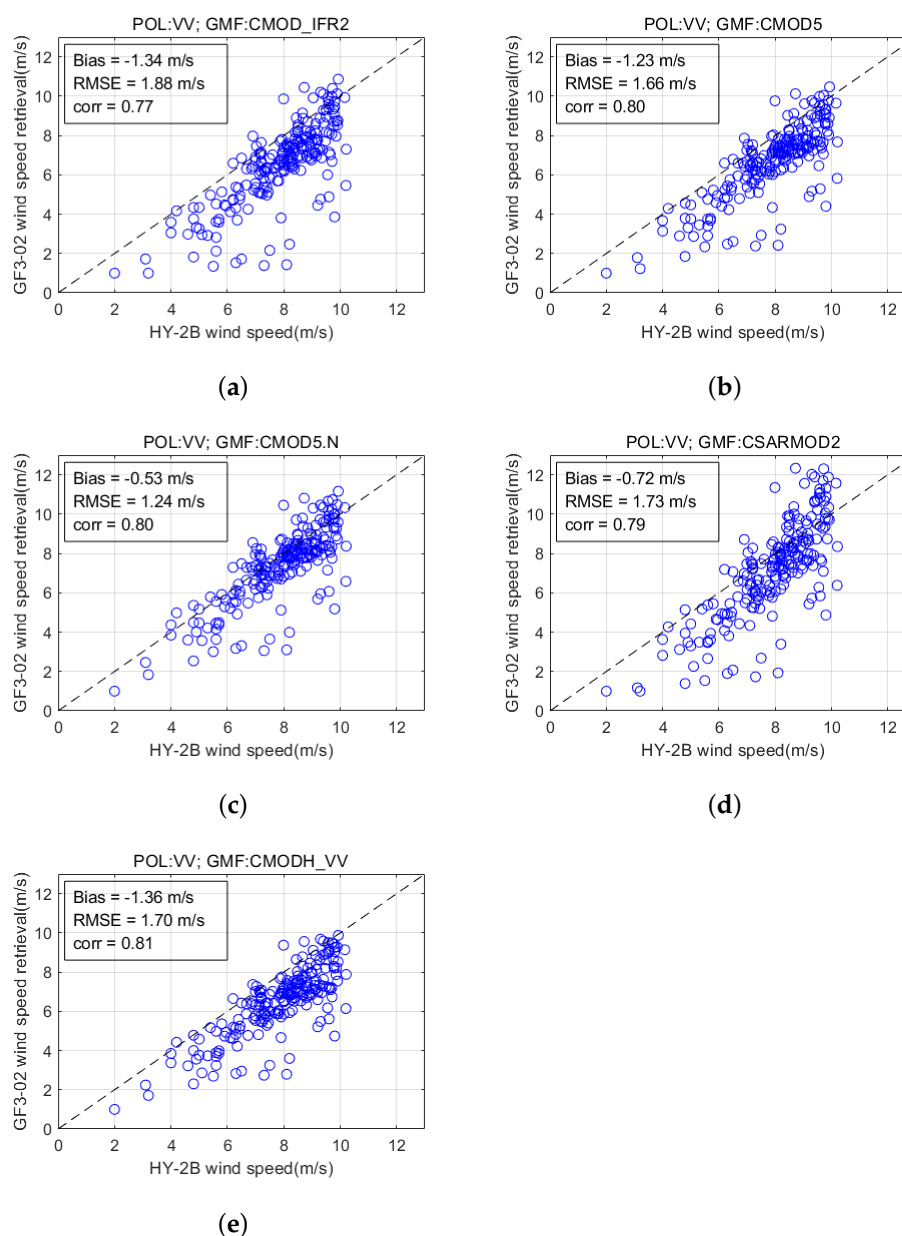


**Figure 5.** Comparison of wind speed retrieval results from GF3-02 VV polarization data based on (a) CMOD\_IFR2, (b) CMOD5, (c) CMOD5.N, (d) CSARMOD2, and (e) CMODH\_VV and HY-2B SCA wind data.

In conclusion, the comprehensive analysis of the wind speed retrieved from the GF3-02 SAR VV polarization data with the NDBC, ERA5, and HY-2B SCA wind speeds shows that CMOD5.N exhibits the overall best performance of the GF3-02 SAR VV polarization. It has the smallest RMSEs of 1.40 m/s, 1.18 m/s, and 1.24 m/s, which can fully meet the operational requirements of GF3-02 SAR. In addition, among the models proposed from SAR data, CMODH\_VV performs better than CSARMOD2 for GF3-02 SAR VV polarization.

### 3.2. GF3-02 SAR Wind Speed from HH Polarization

As shown in Section 3.1, CMOD5.N shows the overall best performance for the GF3-02 SAR VV polarization data. Therefore, for the HH polarization data, the following five models are used: CMOD5.N+PR\_Elfouhaily, CMOD5.N+PR\_Zhang, CMOD5.N+PR\_Ren, CMOD5.N+PR\_Wang, and CMODH\_HH.

### 3.2.1. Compared with NDBC Wind Speed

Figure 3b shows the comparison between wind speed retrieval results from GF3-02 SAR HH polarization data and the matched NDBC wind speed. The RMSE of GF3-02 SAR wind speed retrieval results are 1.87 m/s, 1.39 m/s, 1.72 m/s, 1.81 m/s, and 1.45 m/s, respectively. Based on this, the GF3-02 SAR wind speed retrieval results using the CMOD5.N+PR\_Zhang model are optimal with an RMSE of 1.39 m/s. Moreover, the RMSE of CMODH\_HH is close to the CMOD5.N+PR\_Zhang model.

### 3.2.2. Compared with ERA5 Wind Speed

Figure 6 shows a comparison of the wind speeds obtained by applying the above model to the GF3-02 SAR HH polarization data and the ERA5 reanalysis wind speeds. Table 4 shows the retrieval results of the wind speed of the GF3-02 HH Polarization data based on each GMF model. The RMSE of the retrieved wind speeds are 1.51 m/s, 1.41 m/s, 1.90 m/s, 1.38 m/s, and 1.19 m/s, respectively. It can be clearly seen that the RMSE of CMODH\_HH is the smallest, the deviation is  $-0.40$  m/s, and the correlation coefficient is 0.85. Furthermore, compared with the CMOD5.N for VV polarization, the retrieval accuracy of the HH polarization wind speed using the PR model combined with the CMOD5.N model is poor because there is a certain error in the PR model.

**Table 4.** Comparison of wind speed retrieval results of the GF3-02 HH polarization data based on each GMF model and ERA5 wind data.

GMFs	Bias (m/s)	RMSE (m/s)	Corr
PR_Elfouhaily + CMOD5.N	$-0.81$	1.51	0.80
PR_Zhang + CMOD5.N	$-0.43$	1.41	0.79
PR_Ren + CMOD5.N	$-1.11$	1.90	0.73
PR_Wang + CMOD5.N	$-0.76$	1.38	0.84
CMODH_HH	$-0.40$	1.19	0.85

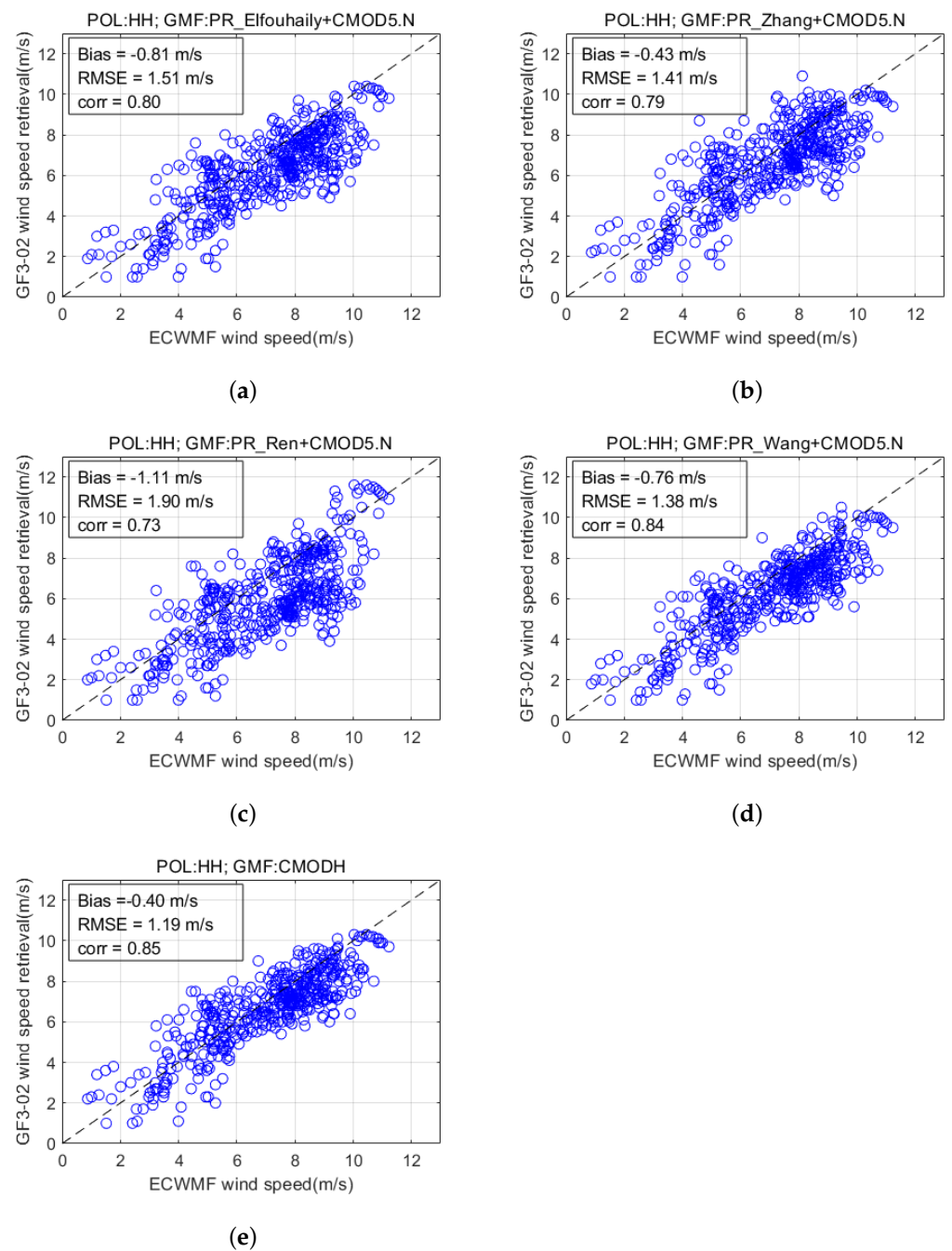
### 3.2.3. Compared with HY-2B SCA Wind Speed

Figure 7 shows a comparison of the wind speeds obtained by applying the above model to the GF3-02 SAR HH polarization data and the HY-2B SCA wind speed. Table 5 shows the retrieval results of the wind speed of the GF3-02 HH Polarization data based on each GMF model. The RMSE of the retrieved wind speeds are 1.91 m/s, 1.70 m/s, 2.58 m/s, 1.67 m/s, and 1.52 m/s, respectively. Consistent with the ERA5 wind speed comparison results, the RMSE of CMODH\_HH is also the smallest, the deviation is  $-1.12$  m/s, and the correlation coefficient is 0.80.

**Table 5.** Comparison of wind speed retrieval results of the GF3-02 HH polarization data based on each GMF model and HY-2B SCA wind data.

GMFs	Bias (m/s)	RMSE (m/s)	Corr
PR_Elfouhaily + CMOD5.N	$-1.62$	1.91	0.80
PR_Zhang + CMOD5.N	$-1.32$	1.70	0.79
PR_Ren + CMOD5.N	$-2.37$	2.58	0.78
PR_Wang + CMOD5.N	$-1.31$	1.67	0.81
CMODH_HH	$-1.12$	1.52	0.80

In conclusion, the comprehensive analysis of the wind speed retrieved from the GF3-02 SAR HH polarization data with the NDBC, ERA5, and the HY-2B SCA wind speeds shows that CMOD\_HH exhibits the overall best performance of the GF3-02 SAR HH polarization. Compared with the three data sets, the RMSE is 1.45 m/s, 1.19 m/s, and 1.52 m/s, which can also meet the operational requirements of GF3-02 SAR.



**Figure 6.** Comparison of wind speed retrieval results from GF3-02 HH polarization data based on (a) CMOD5.N+PR\_Elfouhaily, (b) CMOD5.N+PR\_Zhang, (c) CMOD5.N+PR\_Ren, (d) CMOD5.N+PR\_Wang, and (e) CMODH\_HH and ERA5 wind data.

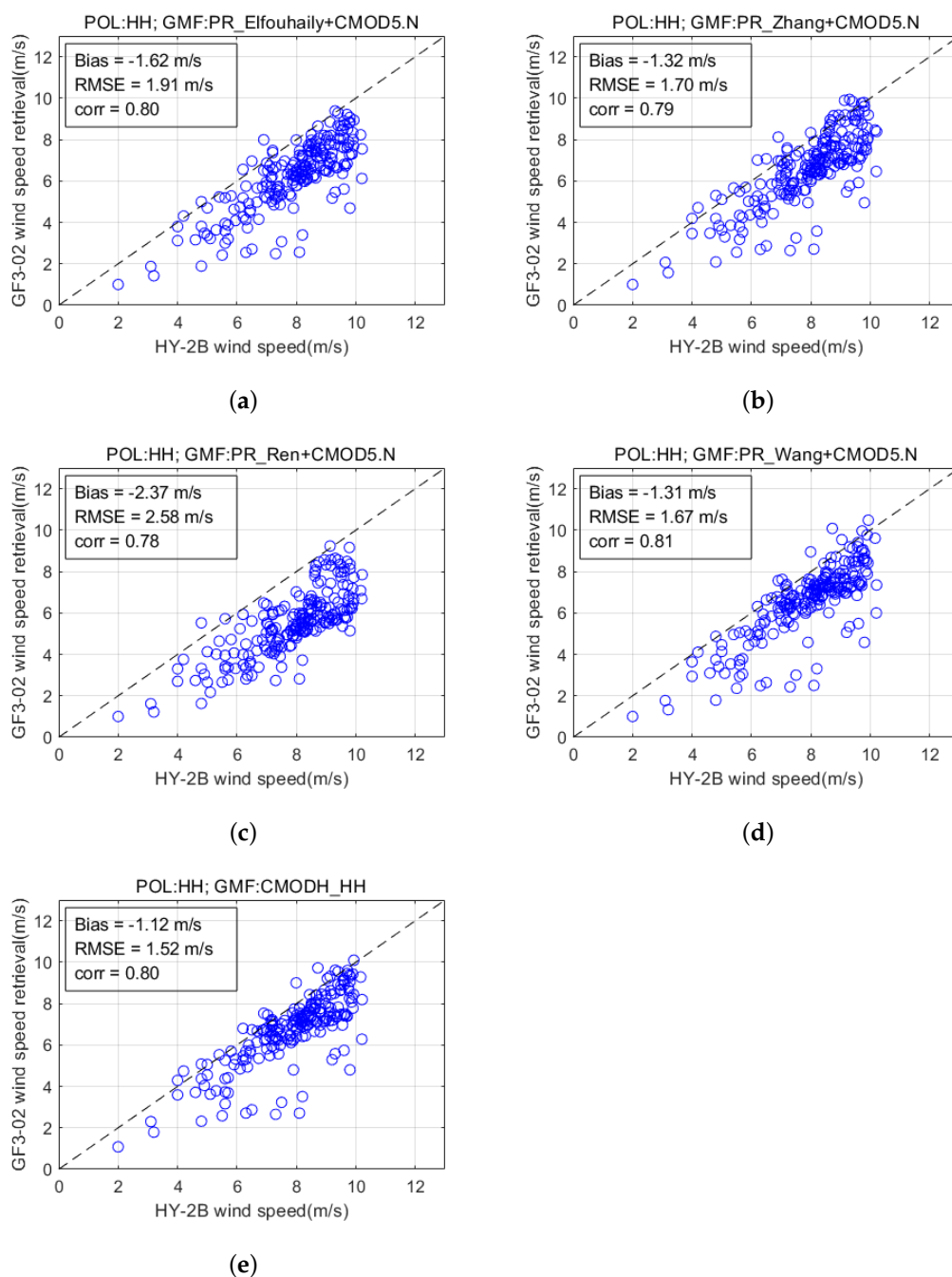


**Figure 7.** Comparison of wind speed retrieval results from GF3-02 HH polarization data based on (a) CMOD5.N+PR\_Elfouhaily, (b) CMOD5.N+PR\_Zhang, (c) CMOD5.N+PR\_Ren, (d) CMOD5.N+PR\_Wang, and (e) CMODH\_HH and HY-2B SCA wind data.

#### 4. Discussion

In this paper, the accuracy of wind speed retrieval of GF3-02 SAR is evaluated for the first time. The SAR wind speed retrieved by different GMF models is compared with NDBC buoy wind speed, ERA5 wind speed, and HY-2B SCA wind speed, respectively. For VV polarization, the optimal RMSE is 1.40 m/s compared with NDBC buoy wind speed, 1.18 m/s compared with ERA5 wind speed, and 1.24 m/s compared with HY-2B SCA wind speed. For HH polarization, the optimal RMSE is 1.39 m/s compared with NDBC buoy wind speed, 1.19 m/s compared with ERA5 wind speed, and 1.52 m/s compared with HY-2B SCA wind speed. The contributions to the RMSE of the wind speed measured by

the GF3-02 SAR are expected in many aspects. Firstly, one of the sources of error is the accuracy of the GF3-02 SAR radiometric calibration. As the GF3-02 SAR external field radiation calibration has not been completed, this paper only uses the Amazon rainforest for preliminary radiation calibration. There may be certain errors in the calibration constants, which directly affect the accuracy of the sea surface NRCS. Secondly, the accuracy of wind speed retrieval largely depends on the GMF model used. After completing the external field radiation calibration, we can further evaluate and optimize the accuracy of the GMF model through a large amount of GF3-02 SAR data. Thirdly, the GF3-02 SAR wind speed retrieval accuracy is limited by the accuracy of the wind speed of the NDBC buoy, ERA5, and HY-2B SCA. The wind speed measured by the buoy can be regarded as the ground truth, but the number of scenes where the SAR data collected in this paper matches the buoy in space is only 10, and the result may be accidental. The collected SAR data are mainly concentrated in the waters near the Hawaiian Islands and the waters off the west coast of the United States, where there are also a large number of NDBC buoys. Therefore, we can verify the accuracy of the ERA5 data by comparing the ERA5 wind speed with the spatially matched NDBC buoy wind speed, thereby indirectly proving the accuracy of the GF3-02 retrieval wind speed results. Figure 8 shows the GF3-02 SAR data and selected NDBC buoys distributed in the waters near the Hawaiian Islands and the waters off the west coast of the United States. Figure 9 shows the comparison results of the ERA5 wind and the NDBC buoys wind at the same time as the SAR imaging moment. Compared with the NDBC buoys wind, the RMSE of the ERA5 wind speed is 1.03 m/s and the RMSE of the wind direction is 18.63°. It is enough to show that the ERA5 wind has high accuracy to verify the retrieval results of the GF3-02 SAR data collected in this paper. In the same way, we matched the wind speed of the HY-2B SCA and the NDBC buoy shown in Figure 8 at the moment of SAR image imaging. The comparison results of the sea surface wind field are shown in Figure 10. Compared with the NDBC buoys wind at the moment of the GF3-02 SAR image, the RMSE of the HY-2B SCA wind speed is 1.64 m/s and the RMSE of the wind direction is 36.07°, which may be affected by individual outliers. In addition, future work is devoted to collecting more GF3-02 SAR data matching the wind field in-site measured data, further analyzing the wind speed retrieval accuracy, and optimizing the wind speed retrieval model.

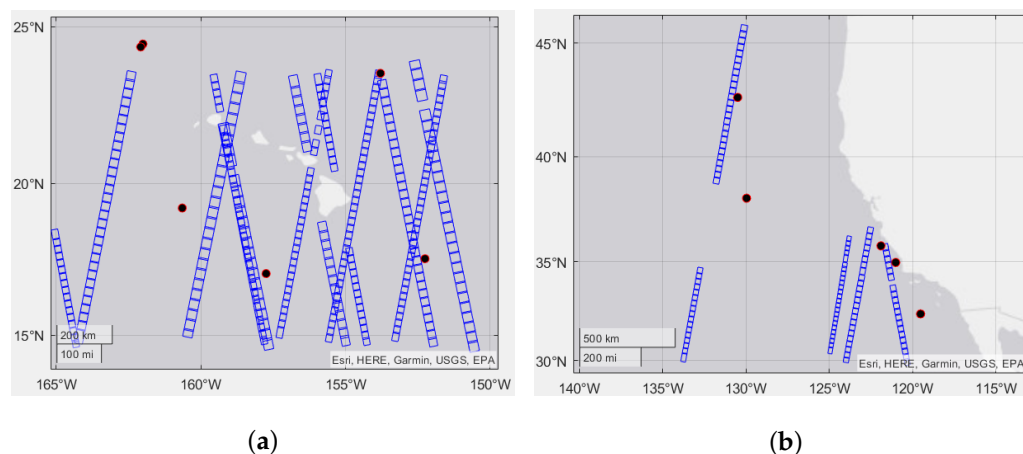


**Figure 8.** The map of SAR data location (Blue boxes) and buoy location of NDBC (black dots) of (a) the waters off the Hawaiian Islands and (b) the waters off the west coast of the United States. The NDBC buoy stations are 51000, 51001, 51002, 51003, 51004, 51101, 46002, 46011, 46028, 46047 and 46059.

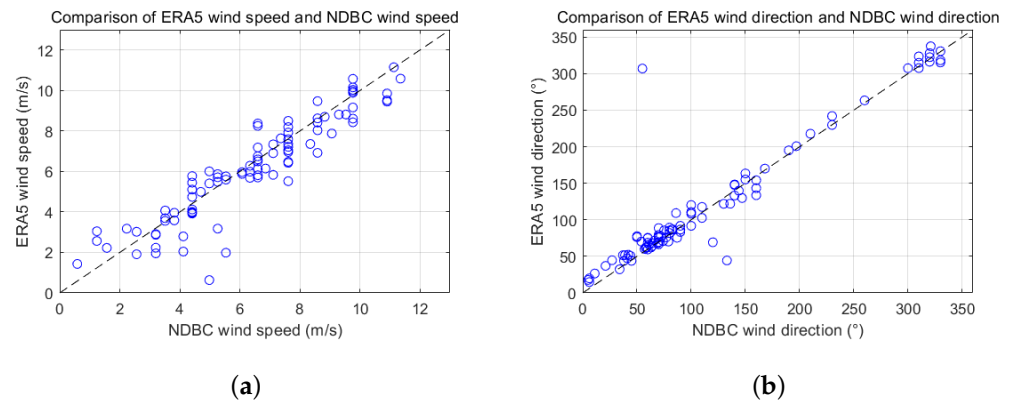


**Figure 9.** Comparison of NDBC buoy wind field and ERA5 wind field. (a) Wind speed comparison results; (b) wind direction comparison results.

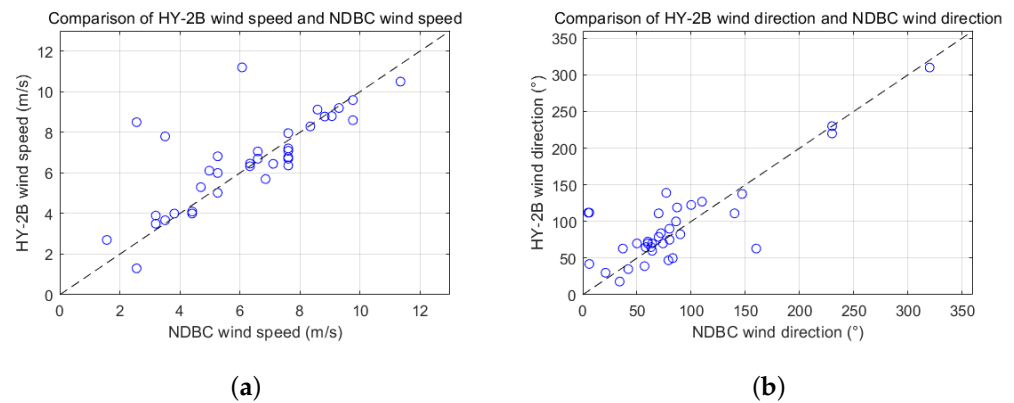


**Figure 10.** Comparison of NDBC buoy wind field and HY-2B SCA wind field. (a) Wind speed comparison results; (b) wind direction comparison results.

## 5. Conclusions

In this paper, the wind speed of the co-polarization obtained by the GF3-02 SAR from January to March 2022 is retrieved, and a more detailed comparative analysis is made with the wind speed measured by buoys of NDBC and ERA5 wind. For the VV polarization, the experimental results show that the optimal wind speed retrieval function is CMOD5.N. Compared with NDBC, ERA5, and HY-2B SCA wind speeds, the RMSE is 1.40 m/s, 1.18 m/s, and 1.24 m/s, respectively. For the HH polarization, the experimental results show that the optimal wind speed retrieval function is the CMODH\_HH model. Compared with NDBC wind speed, ERA5 wind speed, and HY-2B SCA wind speed, the RMSE is 1.45 m/s, 1.19 m/s, and 1.52 m/s, respectively. Furthermore, CMODH\_VV also performs well in wind speed retrieval from GF3-02 SAR VV polarization data. In conclusion, the retrieval results have high precision, which preliminarily verified that GF3-02 SAR has high spatial resolution sea surface wind speed retrieval capability. In addition, the retrieval results show that the GF3-02 Satellite SAR image produced by NSOAS has fine radiation accuracy and radiation stability. Future work will first focus on analyzing the denoising process of GF3-02 SAR cross-polarization to evaluate the performance of GF3-02 SAR cross-polarization to retrieve wind speed. In addition, we will collect more sea surface data of each model of GF3-02 SAR that match the buoy wind fields and reanalysis wind field data and improve the performance evaluation of GF3-02 SAR sea surface wind speed retrieval. Moreover, the GMF is further optimized to improve the operational capability of GF3-02 SAR wind field retrieval.

**Author Contributions:** Conceptualization, J.Y. and B.H.; methodology, J.Y., B.H. and X.W.; software, J.Y. and L.Z.; validation, J.Y. and X.Y.; formal analysis, J.Y.; investigation, X.W.; data curation, J.Y., L.Z. and X.Y.; writing—original draft preparation, J.Y.; writing—review and editing, J.Y. and B.H.; supervision, Y.H. and C.D.; funding acquisition, B.H. All authors have read and agreed to the published version of the manuscript.

**Funding:** This research was funded by the National Natural Science Foundation of China under Grant Number 41976169.

**Acknowledgments:** The GF3-02 SAR products are produced by the NSOAS, and the HY-2B SCA data is provided by the NSOAS through the website <https://osdds.nsoas.org.cn/>, accessed on 1 April 2022 (registration required). The authors thank ECMWF for freely providing the ERA5 wind data via <https://cds.climate.copernicus.eu/>, accessed on 16 February 2022. And we are also grateful for the wind measurements of buoy freely provided by NDBC via <https://www.ndbc.noaa.gov/>, accessed on 1 April 2022.

**Conflicts of Interest:** The authors declare no conflict of interest.

## References

1. Valenzuela, G.R. Theories for the interaction of electromagnetic and oceanic waves—A review. *Bound. Layer Meteorol.* **1978**, *13*, 61–85. [[CrossRef](#)]
2. Long, A. Towards a C-band radar sea echo model for the ERS-1 scatterometer. In Proceedings of a Conference on Spectral Signatures, Les Arcs, France, 16–20 December 1985; pp. 29–34.
3. Stoffelen, A.; Anderson, D. Scatterometer data interpretation: Estimation and validation of the transfer function CMOD4. *J. Geophys. Res. Ocean.* **1997**, *102*, 5767–5780. [[CrossRef](#)]
4. Quilfen, Y.; Chapron, B.; Elfouhaily, T.; Katsaros, K.; Tournadre, J. Observation of tropical cyclones by high-resolution scatterometry. *J. Geophys. Res. Ocean.* **1998**, *103*, 7767–7786. [[CrossRef](#)]
5. Hersbach, H.; Stoffelen, A.; de Haan, S. An improved C-band scatterometer ocean geophysical model function: CMOD5. *J. Geophys. Res. Ocean.* **2007**, *112*, C03006. [[CrossRef](#)]
6. Verhoef, A.; Portabella, M.; Stoffelen, A.; Hersbach, H. CMOD5. n—the CMOD5 GMF for Neutral Winds. 2008. Available online: [https://digital.csic.es/bitstream/10261/156198/1/Verhoef\\_et\\_al\\_2008.pdf](https://digital.csic.es/bitstream/10261/156198/1/Verhoef_et_al_2008.pdf) (accessed on 16 February 2022).
7. Ricciardulli, L.; Meissner, T.; Wentz, F. Towards a climate data record of satellite ocean vector winds. In Proceedings of the 2012 IEEE International Geoscience and Remote Sensing Symposium, Munich, Germany, 22–27 July 2012; pp. 2067–2069.
8. Soisuvann, S.; Jelenak, Z.; Chang, P.S.; Alswiss, S.O.; Zhu, Q. CMOD5. H—A high wind geophysical model function for C-band vertically polarized satellite scatterometer measurements. *IEEE Trans. Geosci. Remote Sens.* **2012**, *51*, 3744–3760. [[CrossRef](#)]
9. Stoffelen, A.; Verspeek, J.A.; Vogelzang, J.; Verhoef, A. The CMOD7 geophysical model function for ASCAT and ERS wind retrievals. *IEEE J. Sel. Top. Appl. Earth Obs. Remote Sens.* **2017**, *10*, 2123–2134. [[CrossRef](#)]
10. Elfouhaily, T. Physical Modeling of Electromagnetic Backscatter from the Ocean Surface, Application to Retrieval of Wind Fields and Wind Stress by Remote Sensing of the Marine Atmospheric Boundary Layer. Ph.D. Thesis, University Paris VII, Paris, France, 1997.
11. Thompson, D.R.; Elfouhaily, T.M.; Chapron, B. Polarization ratio for microwave backscattering from the ocean surface at low to moderate incidence angles. In Proceedings of the IGARSS'98, Sensing and Managing the Environment, 1998 IEEE International Geoscience and Remote Sensing, Symposium Proceedings (Cat. No. 98CH36174), Seattle, WA, USA, 6–10 July 1998; Volume 3, pp. 1671–1673.
12. Zhang, B.; Perrie, W.; Hwang, P.A.; He, Y. A new polarization ratio model from C-Band RADARSAT-2 fine Quad-Pol imagery. In Proceedings of the 2010 IEEE International Geoscience and Remote Sensing Symposium, Honolulu, HI, USA, 25–30 July 2010; pp. 1948–1951.
13. Ren, L.; Yang, J.; Mouche, A.; Wang, H.; Wang, J.; Zheng, G.; Zhang, H. Preliminary analysis of Chinese GF-3 SAR quad-polarization measurements to extract winds in each polarization. *Remote Sens.* **2017**, *9*, 1215. [[CrossRef](#)]
14. Mouche, A.A.; Hauser, D.; Daloze, J.F.; Guérin, C. Dual-polarization measurements at C-band over the ocean: Results from airborne radar observations and comparison with ENVISAT ASAR data. *IEEE Trans. Geosci. Remote Sens.* **2005**, *43*, 753–769. [[CrossRef](#)]
15. Wang, L.; Han, B.; Yuan, X.; Lei, B.; Ding, C.; Yao, Y.; Chen, Q. A preliminary analysis of wind retrieval, based on GF-3 wave mode data. *Sensors* **2018**, *18*, 1604. [[CrossRef](#)]
16. Alpers, W.; Brümmer, B. Atmospheric boundary layer rolls observed by the synthetic aperture radar aboard the ERS-1 satellite. *J. Geophys. Res. Ocean.* **1994**, *99*, 12613–12621. [[CrossRef](#)]
17. Fan, K.; Huang, W.; Chang, J.; Lin, H.; Gu, Y. Sea Surface Wind Speeds Retrieval by SAR Combing with the NCEP/QSCAT Blended Wind Directions. *Remote Sens. Technol. Appl.* **2010**, *25*, 873–876.

18. Zhang, K.; Xu, X.; Han, B.; Mansaray, L.R.; Guo, Q.; Huang, J. The Influence of Different Spatial Resolutions on the Retrieval Accuracy of Sea Surface Wind Speed With C-2PO Models Using Full Polarization C-Band SAR. *IEEE Trans. Geosci. Remote Sens.* **2017**, *55*, 5015–5025. [[CrossRef](#)]
19. Monaldo, F.; Jackson, C.; Li, X.; Pichel, W.G. Preliminary evaluation of Sentinel-1A wind speed retrievals. *IEEE J. Sel. Top. Appl. Earth Obs. Remote Sens.* **2016**, *9*, 2638–2642. [[CrossRef](#)]
20. Wang, H.; Yang, J.; Mouche, A.; Shao, W.; Zhu, J.; Ren, L.; Xie, C. GF-3 SAR ocean wind retrieval: The first view and preliminary assessment. *Remote Sens.* **2017**, *9*, 694. [[CrossRef](#)]
21. Mouche, A.; Chapron, B. Global C-B and E nvisat, RADARSAT-2 and S entinel-1 SAR measurements in copolarization and cross-polarization. *J. Geophys. Res. Ocean.* **2015**, *120*, 7195–7207. [[CrossRef](#)]
22. Lu, Y.; Zhang, B.; Perrie, W.; Mouche, A.A.; Li, X.; Wang, H. A C-band geophysical model function for determining coastal wind speed using synthetic aperture radar. *IEEE J. Sel. Top. Appl. Earth Obs. Remote Sens.* **2018**, *11*, 2417–2428. [[CrossRef](#)]
23. Zhang, B.; Mouche, A.; Lu, Y.; Perrie, W.; Zhang, G.; Wang, H. A geophysical model function for wind speed retrieval from C-band HH-polarized synthetic aperture radar. *IEEE Geosci. Remote Sens. Lett.* **2019**, *16*, 1521–1525. [[CrossRef](#)]
24. Lu, Y.; Zhang, B.; Perrie, W.; Mouche, A.; Zhang, G. CMODH validation for C-band synthetic aperture radar HH polarization wind retrieval over the ocean. *IEEE Geosci. Remote Sens. Lett.* **2020**, *18*, 102–106. [[CrossRef](#)]
25. Han, B.; Ding, C.; Zhong, L.; Liu, J.; Qiu, X.; Hu, Y.; Lei, B. The GF-3 SAR data processor. *Sensors* **2018**, *18*, 835. [[CrossRef](#)]